AFRL-RZ-WP-TP-2012-0102

GROWTH OF YBCO THIN FILMS ON TiN(001) AND CeO_2-COATED TiN SURFACES (POSTPRINT)

Paul N. Barnes, Rand Biggers, Gregory Kozlowski, Chakrapani Varanasi, Iman Maartens, Rama Nekkanti, Tim Peterson, and Timothy J. Haugan

Mechanical Energy Conversion Branch
Energy/Power/Thermal Division

Ilwon Kim, Scott A. Barnett, and Sankar Sambasivan

Applied Thin Films, Inc.

Amit Goyal

Oak Ridge National Laboratory

FEBRUARY 2012

AIR FORCE RESEARCH LABORATORY
PROPULSION DIRECTORATE
WRIGHT-PATTERSON AIR FORCE BASE, OH 45433-7251
AIR FORCE MATERIEL COMMAND
UNITED STATES AIR FORCE

REPORT DOCUMENTATION PAGE

Form Approved
OMB No. 0704-0188

1. REPORT DATE *(DD-MM-YY)*	2. REPORT TYPE	3. DATES COVERED *(From - To)*
February 2012	Journal Article Postprint	01 September 2000 – 01 September 2002

4. TITLE AND SUBTITLE

GROWTH OF YBCO THIN FILMS ON TiN(001) AND CeO_2-COATED TiN SURFACES (POSTPRINT)

5a. CONTRACT NUMBER
In-house

5b. GRANT NUMBER

5c. PROGRAM ELEMENT NUMBER
62203F

6. AUTHOR(S)

Paul N. Barnes, Rand Biggers, Gregory Kozlowski, Chakrapani Varanasi, Iman Maartens, Rama Nekkanti, Tim Peterson, and Timothy J. Haugan (AFRL/RZPG)
Ilwon Kim, Scott A. Barnett, and Sankar Sambasivan (Applied Thin Films, Inc.)
Amit Goyal (Oak Ridge National Laboratory)

5d. PROJECT NUMBER
3145

5e. TASK NUMBER
32

5f. WORK UNIT NUMBER
314532Z9

7. PERFORMING ORGANIZATION NAME(S) AND ADDRESS(ES)

Mechanical Energy Conversion Branch (AFRL/RZPG)
Energy/Power/Thermal Division
Air Force Research Laboratory, Propulsion Directorate
Wright-Patterson Air Force Base, OH 45433-7251
Air Force Materiel Command, United States Air Force

Applied Thin Films, Inc.
Evanston, IL 60201

Oak Ridge National Laboratory
Oak Ridge, TN 37831

8. PERFORMING ORGANIZATION REPORT NUMBER
AFRL-RZ-WP-TP-2012-0102

9. SPONSORING/MONITORING AGENCY NAME(S) AND ADDRESS(ES)

Air Force Research Laboratory
Propulsion Directorate
Wright-Patterson Air Force Base, OH 45433-7251
Air Force Materiel Command
United States Air Force

10. SPONSORING/MONITORING AGENCY ACRONYM(S)
AFRL/RZPG

11. SPONSORING/MONITORING AGENCY REPORT NUMBER(S)
AFRL-RZ-WP-TP-2012-0102

12. DISTRIBUTION/AVAILABILITY STATEMENT

Approved for public release; distribution unlimited.

13. SUPPLEMENTARY NOTES

Journal article published in *Physica C*, Vol. 377, 2002. Work on this effort was completed in 2002.
PA Case Number: ASC-01-1691; Clearance Date: 19 Nov 2002. This paper contains color

14. ABSTRACT

Epitaxial growth of $YBa_2Cu_3O_{7-x}$ (YBCO) layers on TiN(0 0 1) surfaces was explored, both with and without CeO_2 intermediate layers. The epitaxial TiN layers were grown on MgO(0 0 1) and textured Ni substrates. Thin CeO_2 (~200 nm thick) and YBCO (~300 nm thick) layers were grown on TiN-coated MgO substrates, using pulsed laser deposition. While YBCO grown directly on TiN was of poor quality, a good epitaxial YBCO layer was obtained using a thin CeO_2 cap layer on the TiN. A superconducting critical transition temperature (T_c) of 89 K was measured by AC susceptibility. The critical current density (J_c) was 6×10^5 A/cm^2 obtained at 77 K by whole body transport current measurement in self-field using a 1 μV/cm criteria. These results suggest that transition metal nitrides, such as TiN, are potentially useful as buffer layers for YBCO thin films. Advantages of the nitride buffer layers compared to conventional oxide buffers include high electrical and thermal conductivity, better mechanical toughness, good diffusion barrier characteristics, and relative ease of deposition.

15. SUBJECT TERMS

high-temperature superconductors, $BaSnO_3$, critical current density, superconducting transition temperature, $YBa_2Cu_3O_{7-\delta}$

16. SECURITY CLASSIFICATION OF:			17. LIMITATION OF ABSTRACT:	18. NUMBER OF PAGES	19a. NAME OF RESPONSIBLE PERSON (Monitor)
a. REPORT	b. ABSTRACT	c. THIS PAGE			Timothy J. Haugan
Unclassified	Unclassified	Unclassified	SAR	14	19b. TELEPHONE NUMBER *(Include Area Code)* N/A

ELSEVIER

Physica C 377 (2002) 227–234

PHYSICA C

www.elsevier.com/locate/physc

Growth of YBCO thin films on TiN(0 0 1) and CeO_2-coated TiN surfaces

Ilwon Kim [a], Paul N. Barnes [b,*], Amit Goyal [c], Scott A. Barnett [a], Rand Biggers [b], Gregory Kozlowski [b], Chakrapani Varanasi [b], Iman Maartens [b], Rama Nekkanti [b], Tim Peterson [b], Tim Haugan [b], Sankar Sambasivan [a]

[a] *Applied Thin Films, Inc., Evanston, IL 60201, USA*
[b] *Air Force Research Laboratory/PRPG, Bldg. 450, 2645 Fifth St., Ste. 13, Wright-Patterson AFB, OH 45433-7919, USA*
[c] *Oak Ridge National Laboratory, Oak Ridge, TN 37831, USA*

Received 2 August 2001; received in revised form 9 October 2001; accepted 26 October 2001

Abstract

Epitaxial growth of $YBa_2Cu_3O_{7-x}$ (YBCO) layers on TiN(0 0 1) surfaces was explored, both with and without CeO_2 intermediate layers. The epitaxial TiN layers were grown on MgO(0 0 1) and textured Ni substrates. Thin CeO_2 (~200 nm thick) and YBCO (~300 nm thick) layers were grown on TiN-coated MgO substrates, using pulsed laser deposition. While YBCO grown directly on TiN was of poor quality, a good epitaxial YBCO layer was obtained using a thin CeO_2 cap layer on the TiN. A superconducting critical transition temperature (T_c) of 89 K was measured by AC susceptibility. The critical current density (J_c) was 6×10^5 A/cm^2 obtained at 77 K by whole body transport current measurement in self-field using a 1 μV/cm criteria. These results suggest that transition metal nitrides, such as TiN, are potentially useful as buffer layers for YBCO thin films. Advantages of the nitride buffer layers compared to conventional oxide buffers include high electrical and thermal conductivity, better mechanical toughness, good diffusion barrier characteristics, and relative ease of deposition.
Published by Elsevier Science B.V.

PACS: 74.72.B; 74.76.B; 74.70.A
Keywords: $YBa_2Cu_3O_{7-\delta}$; TiN; Nitride buffer layers; HTS coated conductors

1. Introduction

High temperature superconducting (HTS) $YBa_2Cu_3O_{7-x}$ (YBCO) films grown on metallic substrates, i.e. YBCO coated conductors, presently require epitaxial buffer layers between the superconducting film and the substrate to prevent reaction with the substrates or diffusion of the metal constituents into the YBCO [1–3]. Critical current densities of $J_c > 1 \times 10^6$ A/cm^2 at 77 K, self-field, have been reported when yttria-stabilized zirconia (YSZ) and CeO_2 are used as buffer layers [1–3]. Both YSZ and CeO_2 serve as good epitaxial buffer

* Corresponding author. Tel.: +1-937-255-4410; fax: +1-937-656-4095.
E-mail address: paul.barnes@wpafb.af.mil (P.N. Barnes).

0921-4534/01/$ - see front matter Published by Elsevier Science B.V.
PII: S0921-4534(01)01200-X

Table 1
Properties of refractory cubic nitrides

Material	Cell constant (Å)	CTE (ppm/°C)	Thermal conductivity (W/m K)	Young's modulus (GPa)	Micro-hardness (Kg/mm^2)	Electrical resistivity ($\mu\Omega$ cm)
TiN	4.235	8.1	22	600	2000	20–30
VN	4.14	8.1	5.2	460	1500	85
HfN	4.526	6.5	17		1600	32
NbN	4.39	10		480	1400	58
Ni	3.524	11				
YBCO	3.86	13				

layers because of their relatively close lattice match with the YBCO and with the nickel substrates, good diffusion barrier characteristics, and chemical compatibility with YBCO.

While these rare earth oxides satisfy the key buffer layer criteria mentioned above, they may not be optimal for coated conductor applications. Additional properties desired include high mechanical strength and toughness to prevent cracking, and high electrical (some applications) and thermal conductivity. The ease of buffer layer deposition is a critical factor, since it is a challenging engineering task to develop a large-scale continuous process for producing crack-free and pore-free oxide films of the necessary thickness at reasonable deposition rates [4].

Oxide buffer layers are also not optimal for the case of YBCO on Si substrates for electronics applications. The coefficient of thermal expansion (CTE) mismatch of the oxides with Si is relatively large, reducing the thickness of YBCO to be grown without cracking [5]. As with Ni substrates, the oxidation of silicon during processing limits deposition techniques to those that can maintain low to no oxygen partial pressure [6–8]. Besides the above considerations, there may be in certain circumstances a desire for the buffer layer to be electrically conducting for a direct current path between the YBCO and substrate. For some HTS coated conductor applications, coupling between the YBCO and Ni can be used to electrically stabilize the conductor during transient loss of superconductivity in places.

These factors suggest that other buffer layer materials with potentially superior properties should be explored. One class of materials that possesses many of the desired properties is the transition metal nitrides. Many of these nitrides have high electrical conductivity, better mechanical toughness than the oxides, and are also relatively easy to grow at high rates by reactive sputtering [9]. In addition, some of these nitrides possess thermal expansion coefficients between those of Si and YBCO. Table 1 shows some relevant physical properties of typical transition metal nitrides.

Here, we demonstrate the feasibility of TiN as an alternate buffer material for YBCO thin films. TiN is widely used as a wear resistive coating for tools and as a diffusion barrier in integrated circuits. High rate and large area deposition by reactive magnetron sputtering is well established for TiN [10]. There are only a few previous reports on TiN buffer layers for YBCO [11,12]. However, the J_c values were relatively low, approximately 9.0×10^4 A/cm^2 at 77 K and zero magnetic field, and only a limited microstructural study was done [11]. The other reference dealt only with TiN as a barrier using $YBa_{1.5}Cu_3O_{7-x}$; properly textured $YBa_2Cu_3O_{7-x}$ was not applied as indicated in Ref. [12].

2. Experimental

Epitaxial TiN films were deposited on MgO-(0 0 1) substrates and textured Ni substrates. MgO was chosen as the initial substrate due to its excellent lattice match with TiN. The TiN was deposited using an ultra-high vacuum, dc reactive magnetron sputtering system that was described elsewhere [13]. The MgO(0 0 1) substrates were ultrasonically cleaned in 1,2-dichloroethylene first, while the textured Ni was degreased with chloro-

form. The substrates were then subsequently cleaned in acetone and methanol, and finally blown with a jet of dry N_2 before insertion into the chamber. Immediately prior to deposition, the substrates were heated in a vacuum to approximately 600–700 °C for desorption of surface contaminants. The growth was carried out in Ar–N_2 mixtures (gas purities $> 99.999\%$) at total pressures between 12 and 15 mTorr. The sputtering target used was 5 cm diameter disk consisting of 99.95% pure Ti. The typical growth temperature used for TiN on MgO was ~750 °C. TiN growth on the textured Ni was done at growth temperatures ranging between 300 and 800 °C. The deposition rates were measured by masking a part of the MgO substrate with a small strip of Ta foil, and measuring the thickness of the resulting step edge using a stylus profilometer. Typical thickness of the TiN films were ~300 nm.

The coated TiN layers were characterized by X-ray diffraction (XRD) and optimized with respect to the rocking curve full-width-half-maximums (FWHM) from TiN(0 0 1) out-of-plane peak. For some samples, an ~200 nm thick CeO_2 layer was grown on the TiN-coated MgO and then an ~300 nm thick YBCO layers was subsequently deposited. For other samples, YBCO deposition directly on the TiN was also attempted. Pulsed laser deposition (PLD) was used for deposition of CeO_2 and YBCO. PLD was conducted using a Lambda Physik LPX 305i excimer laser with the KrF transition, $\lambda = 248$ nm and a 25 ns pulse width. The laser fluence was 0.8 $J\,cm^{-2}$. Samples were mounted onto the heater block in the deposition chamber with silver paint. The heater block was positioned opposite to and approximately 7.5 cm from the target. The substrate holder was heated to ~760 °C and maintained at this temperature during deposition. The chamber was pumped to a base pressure of 10^{-5} Torr and then maintained at a pressure of 150 mTorr of O_2 for the YBCO and CeO_2 deposition. In some cases, the CeO_2 growth was initiated in 150 mTorr of Ar (5% H_2) and then continued under an 150 mTorr O_2 pressure. The films, both YBCO and CeO_2, were grown at a 4 Hz laser pulse repetition rate. After deposition, the samples were cooled from 760 to 400 °C over half an hour in 150 mTorr O_2 pressure and then maintained at 400 °C for half an hour in 400 Torr O_2 pressure. Samples were removed after cooling to <100 °C in the chamber with no heating.

The critical transition temperature (T_c) of YBCO was measured by ac susceptibility and the critical current density (J_c) by the four-probe transport current measurement. Selected TiN layers on textured Ni were characterized with a high resolution scanning electron microscopy (SEM) for an electron backscattered Kikuchi diffraction (BKD) image from the surface. Orientation imaging micrographs (OIM) were obtained in a hexagonal grid with a step size of 4 μm from the surface of the TiN layer. Patterns were obtained from every macroscopic region of the substrate, $\sim 1 \times 1$ mm^2, and corresponded to over 200,000 diffraction patterns. At each point the pattern was indexed to give an unique measure of the three-dimensional orientation. A hypothetical hexagonal grid was then superimposed on the pattern grid and all resulting grain boundary misorientations were calculated.

The XRD scans were done on a four-circle diffractometer. The diffractometer was equipped with a Ni-filter in the incident beam. θ–2θ-scans and phi-scans were routinely performed to verify the biaxial texture of all the samples. Use of the MgO single crystal substrate allowed an assessment of the growth-induced misalignment for YBCO on buffers without any additional broadening from textured polycrystalline metal tape.

3. Results

3.1. Epitaxial YBCO and CeO_2 on TiN-coated MgO single crystals

Direct growth of YBCO on the TiN buffered substrates typically resulted in YBCO films with poor quality. The better samples still had critical currents (I_c) less than 1 A and magnetic susceptibility indicated ΔTs generally greater than 10°. XRD 2θ–θ-scans of the films indicated the formation of titanium oxide. This suggested that the main factor preventing good growth of the YBCO was oxidation of the TiN films during deposition. Using a thin intermediate CeO_2 layer allowed this

problem to be largely circumvented. YBCO films with a good epitaxial quality were obtained on a CeO_2 intermediate layer when the CeO_2 growth was initiated in 150 mTorr of Ar (5% H_2) and continued with growth of the CeO_2 in an 150 mTorr O_2 pressure.

Typical FWHM of the XRD 2θ–θ-scan rocking curve peaks were ~0.1° for MgO and ~0.15° for TiN on the MgO grown at ~750 °C. The quality of the TiN films slowly degraded as the growth temperature was increased over 800 °C or decreased much below than 750 °C, consistent with previous reports on epitaxial growth of TiN on MgO [14]. The positions of the phi-scan peaks indicated cube-on-cube epitaxy of the CeO_2 and the TiN with respect to the MgO substrate, while the YBCO was rotated 45° along ⟨0 0 1⟩ with respect to the CeO_2. These measurements were consistent with previous studies of YBCO on CeO_2 buffers [1–3], and TiN film on MgO substrates [14]. The FWHM values of the phi-scan TiN(2 2 0) peaks were ~0.5°, while for MgO(2 2 0) they were typically ~0.3–0.4°. Pole figure analysis showed an in-plane misorientation of less than 8° for YBCO, while the out-of-plane misorientation was <1° for YBCO indicating a well-aligned biaxial texture. Notice that the quality of the YBCO layer was still reasonable, considering a large lattice mismatch between TiN and CeO_2 (24.6%).

Fig. 1(a) shows AC susceptibility vs. temperature at H-field. The superconducting transition temperature (T_c) was 89 K, while the transition width was ~2 K. Fig. 1(b) shows results of whole body transport current measurements carried out at 77 K on a typical YBCO film with the CeO_2 intermediate layer. A critical current (I_c) of 10.26 A was observed. The calculated J_c values for the sample was $\sim 6.5 \times 10^5$ A/cm^2 at 77 K in self-field using the 1 μV/cm criteria.

3.2. Epitaxial growth of TiN on Ni

The TiN films were grown on textured Ni at growth temperatures (T_s) ranging from 300 to 800 °C. The films grown at T_s between 550 and 650 °C showed (0 0 1) orientation in the out-of-plane direction and biaxial-texture in the in-plane direction. A lower or higher T_s resulted in films with (1 1 1) out-of-plane orientation or a random orientation. This is probably due to a large lattice mismatch between Ni and TiN (18.6%).

Sputtered TiN films grown on the textured nickel substrates displayed an excellent in-plane and out-of-plane alignment. Fig. 2 shows a TiN-(1 1 1) pole figure for one of the samples. The TiN(1 1 1) phi-scan showed a FWHM of 6.6°, obtained by Gaussian fit to the data. This FWHM was slightly better than that of the underlying Ni with a FWHM of ~7°. The rocking curve FWHM values from the out-of-plane (0 0 1) reflection of the TiN layer were 3.2° and 6.6° in and about the rolling direction. These were almost 2° sharper than the underlying Ni substrate.

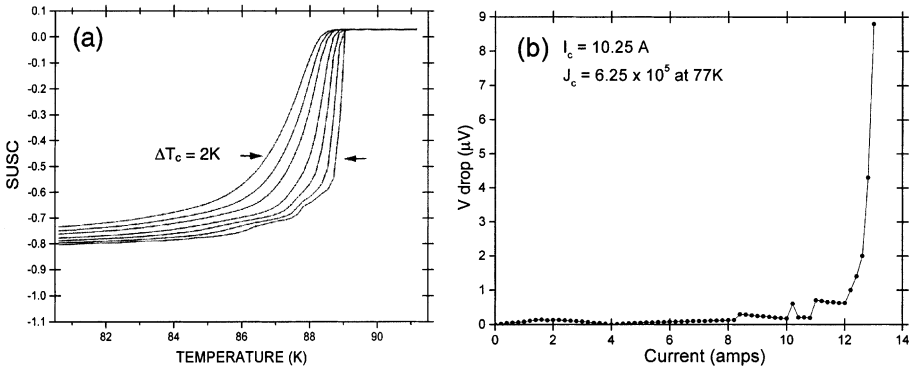

Fig. 1. (a) AC susceptibility vs. temperature at varied H-field and (b) whole body transport current measurement for a YBCO/CeO_2/TiN/MgO sample.

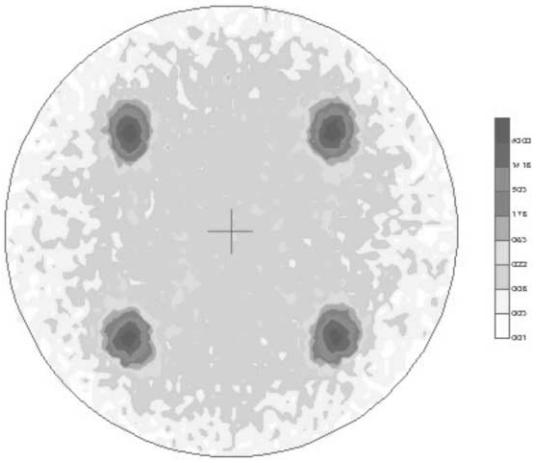

Fig. 2. TiN(1 1 1) pole figure for a 300 nm thick TiN layer deposited on textured Ni using high-rate reactive sputtering. The figure uses a log scale to clearly indicate the single orientation.

Fig. 3(a) shows an electron BKD image from the surface of the TiN on Ni. The grain structure of the TiN resembles that of the Ni substrate below. Variations in intensity in the figure are a reflection of pattern quality or intensity of the Kikuchi bands. Since BKD patterns from grain boundaries result in two superimposed patterns, grain boundaries in the sample are darker. Grain to grain contrast is a reflection of electron channeling contrast in this highly textured sample. Fig. 3(b) shows (1 1 1), (1 0 0) and (1 1 0) pole figures corresponding to the orientation data obtained from the region corresponding to Fig. 3(a). Fig. 4(a) and (b) shows the intensity of the (1 1 1) and (2 0 0) poles in the pole figures corresponding to Fig. 3(b). The FWHM of both the (1 1 1) pole plot corresponding to the in-plane texture and of the (1 0 0) plot corresponding to the out-of-plane texture are consistent with the macroscopic X-ray texture.

Fig. 5 shows the grain boundary misorientations in the TiN layer displayed by the coloring of the same region as shown in Fig. 3(a). Fig. 6 shows the color-coded grain boundaries superimposed on the image shown in Fig. 3(a). Three types of grain boundaries are indicated in the figure: green boundaries denote boundaries with misorientations greater than 1° and less than 5°, yellow lines denote boundaries with misorientations greater than 5° and less than 10°, while red boundaries

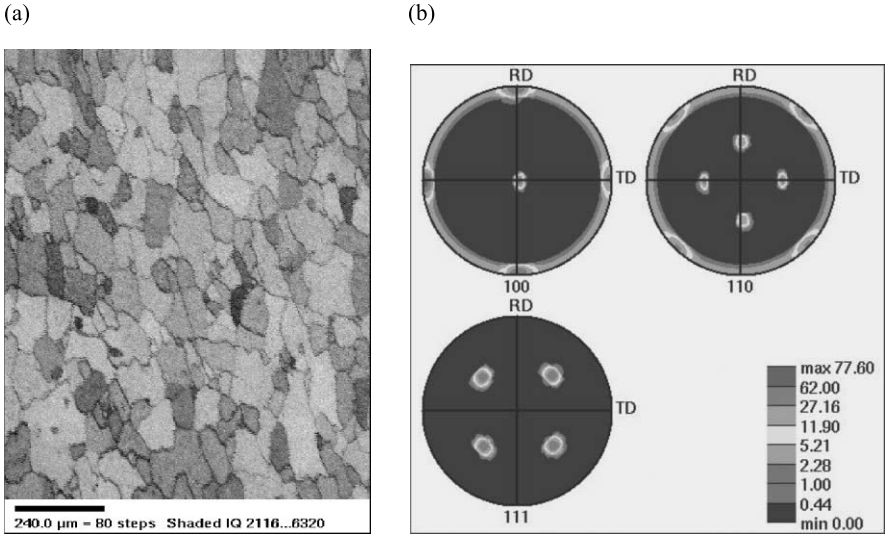

Fig. 3. (a) OIM obtained in a hexagonal grid with a step size of 4 μm. Patterns are obtained solely from orientation data. Since BKD patterns from grain boundaries result in two superimposed patterns, grain boundaries in the sample are darker. Also, grain to grain contrast is a reflection of electron channeling contrast. (b) shows (1 1 1), (1 0 0), and (1 1 0) pole figures corresponding to the orientation data obtained from the region shown in Fig. 3(a).

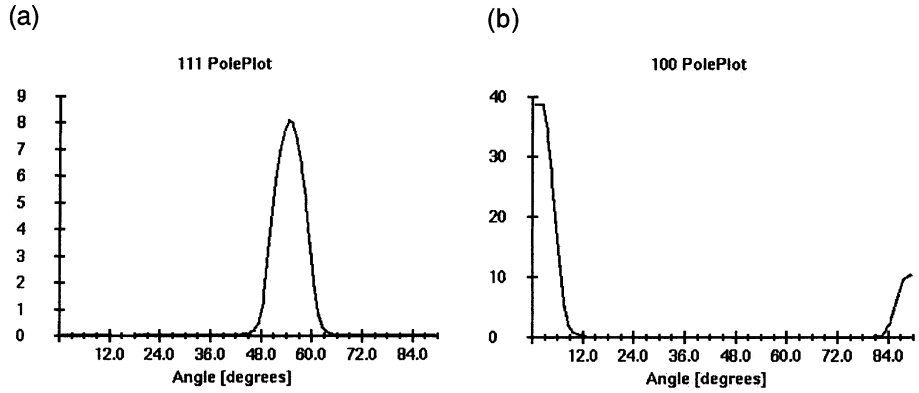

Fig. 4. (a) TiN(1 1 1) pole plot, and (b) TiN(1 0 0) pole plot obtained from Fig. 5(b).

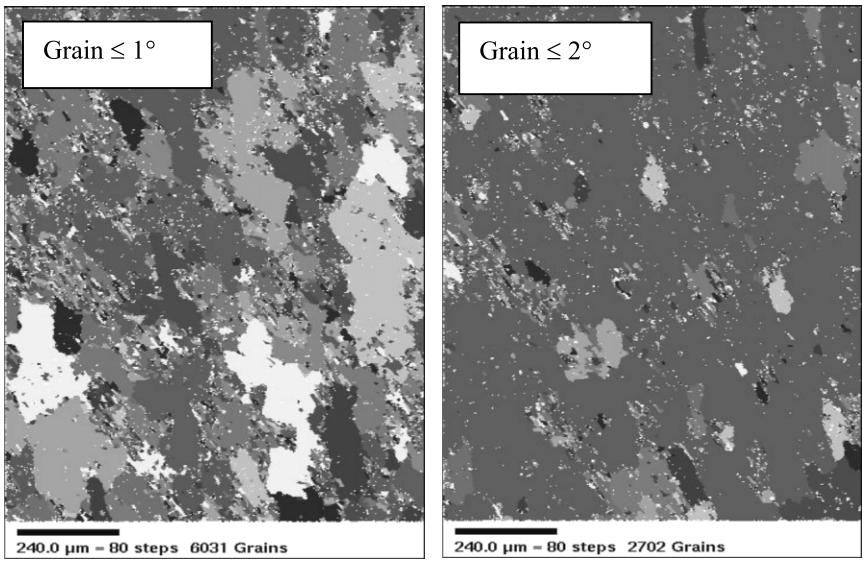

Fig. 5. OIM corresponding to Fig. 3(a), with the grains shaded so that a single shade represents a contiguous or percolative region of orientation change of less than 1° and 2° respectively.

denote boundaries with misorientations greater than 10°. The mapping indicates that primarily low angle boundaries are present.

Fig. 7 shows a scanning electron micrograph from the surface of ~0.5 μm thick TiN on Ni. No evidence of microcracking was seen. Even for the case of thicker TiN layers, no cracks were observed. The contrast observed in the micrograph is a result of the grain boundary structure of the underlying textured Ni substrate.

4. Discussion

As the TiN suffered from oxidation at typical growth temperatures of YBCO (~700–800 °C), the YBCO films grown directly on the TiN-coated MgO exhibited poor quality with relatively low T_c and J_c values. Based on this result, it may be inferred that YBCO is not chemically compatible with TiN for typical YBCO deposition temperatures. However, experimental evidence for TiN–

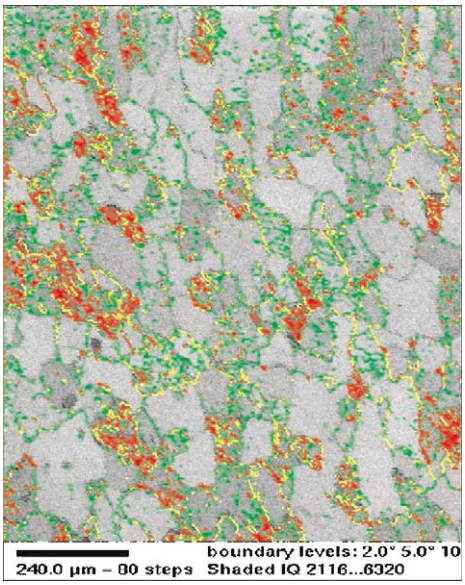

Fig. 6. OIM from Fig. 5 with superimposed color-coded grain boundaries.

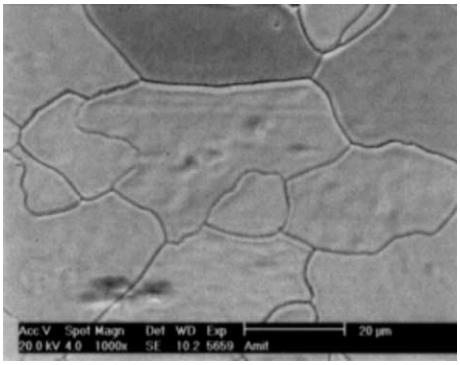

Fig. 7. High magnification scanning electron micrograph of the surface of TiN deposited epitaxially on biaxially textured Ni.

YBCO compatibility was reported in an earlier study where TiN coatings were deposited on hastelloy substrates with an overcoat of YBCO deposited at 600 °C [11]. A T_c value of 85 K obtained for the YBCO film provides some indirect evidence for the TiN–YBCO compatibility [11].

Good epitaxial YBCO was obtained when a thin over layer of CeO_2 was deposited on the TiN/MgO. This demonstrates the potential of TiN as at least a good primary buffer, if not a single, stand alone buffer. Although the feasibility of the CeO_2 intermediate layer was demonstrated for epitaxial YBCO, high J_c values (over 5×10^5 A/cm^2) from YBCO/thin CeO_2/TiN/MgO was not consistently reproduced. Thus thin layers of other oxides materials may prove more beneficial. For conductor applications where an electrically conducting path to the substrate is desired, the use of an insulating oxide layer such as CeO_2 would obviate any advantage of the conducting TiN buffer layer. It may be possible to reduce the oxide thickness, allowing electrical tunneling from YBCO to TiN, or consider other thin conducting buffers in lieu of the insulating oxide layer.

5. Conclusions

YBCO films with good biaxial texture were grown on TiN-coated MgO substrates. Thin CeO_2 intermediate layers were needed for high J_c and T_c of the YBCO. It is not clear what the minimum thickness of the CeO_2 intermediate layer can be for subsequent growth of high quality YBCO. Excellent epitaxy of TiN was obtained on the biaxially textured Ni substrate using high-rate, reactive magnetron sputtering. The out-of-plane texture of the TiN layer was improved over the starting Ni substrate. Furthermore, the TiN films were smooth with no evidence of any microcracking, indicating the potential of the TiN as a primary buffer layer for YBCO. This combined with a relatively high J_c in the YBCO on the CeO_2 capped TiN films implies the feasibility of TiN as a primary buffer layer with a thin cap layer, but inconclusively as a single buffer layer. While the J_c and T_c values obtained were lower than those of YBCO grown on epitaxial YSZ and CeO_2 buffer layers, further improvements are expected upon optimization of the intermediate oxide layer.

Acknowledgements

This work was supported by the Air Force Office of Scientific Research and the Ballistic Missile Defense Organization under the Small Business Innovation Research Program contract

no. F33615-99-C-2884. Work at the Oak Ridge National Laboratory, managed by UT-Battelle, LLC was performed for the U.S. Department of Energy under contract no. DEAC-05-00OR22725.

References

[1] Y. Iijima, H. Hayakawa, N. Sadakata, O. Kohno, Proc. MT-11, Tsukuba, Japan, 1988, p. 1442.
[2] X.D. Wu, S.R. Foltyn, P.N. Arendt, J. Townsend, C. Adams, I.H. Campbell, P. Tiwari, J.Y. Coultier, D.E. Petersen, Appl. Phys. Lett. 65 (1994) 1961.
[3] A. Goyal, D.P. Norton, J.D. Budai, M. Paranthaman, E.D. Specht, D.M. Kroeger, D.K. Christen, Q. He, B. Saffian, F.A. List, D.F. Lee, P.M. Martin, C.E. Klabunde, E. Hatfield, V.K. Sikka, Appl. Phys. Lett. 69 (1996) 1795.
[4] M. Paranthaman, A. Goyal, F.A. List, E.D. Specht, D.F. Lee, P.M. Martin, Q. He, D.K. Christen, D.P. Norton, J.D. Budai, Physica C 275 (1997) 266.
[5] R. Haakenaasen, D.K. Fork, J.A. Golovchenko, Appl. Phys. Lett. 64 (1994) 1573.
[6] A.N. Tiwari, S. Blunier, H. Zogg, P. Lerch, F. Marcenat, P. Martinoli, J. Appl. Phys. 71 (1992) 5095.
[7] D.K. Fork, G.A. Connell, J.B. Boyce, T.H. Geballe, Physica C 185 (1991) 2117.
[8] J.M. Qiao, C.Y. Yang, Mater. Sci. Eng. R 14 (1995) 157.
[9] J.E. Sundgren, H.T.G. Hentzell, J. Vac. Sci. Technol. A 4 (1986) 2259.
[10] W.D. Sproul, W.D. Sproul, J.E. Greene, J.A. Thornton (Eds.), Physics and Chemistry of Protective Coatings, AIP Conf. Proc., vol. 149, 1986, p. 157.
[11] A. Kumar, J. Narayan, X. Chen, Appl. Phys. Lett. 61 (1992) 976;
A. Kumar, J. Narayan, Supercond. Sci. Technol. 6 (1993) 662.
[12] K.G. Grigorov, G.I. Grigorov, M.V. Stoyanova, R.A. Chakalov, J.-L. Vignes, J.-P. Langeron, P. Denjean, J. Perriere, Vacuum 44 (1993) 1119.
[13] P.B. Mirkarimi, M. Shinn, S.A. Barnett, J. Vac. Sci. Technol. A 10 (1992) 1618;
I.W. Kim, Z. Liu, S. Sambasivan, S.A. Barnett, A. Goyal, M. Paranthaman, C. Park, P.N. Barnes, Growth of YBCO film on TiN/biaxially textured Ni, draft.
[14] L. Hultmnan, S.A. Barnett, J.E. Sundgren, J.E. Greene, J. Cryst. Growth 92 (1988) 639.